Even if a liquid-liquid system of low-value interaction rate (hence a stabilized droplets system) were used, the rest-time of reacting droplets in the course of stopping the reaction would be increased, and that increased rest-time would induce error in the measurement of reaction conversion. This would be a limitation involved in the experimental study.

Conclusion

It is demonstrated that the interaction rates measured by a chemical reaction are in agreement with those directly measured by a physical method within experimental accuracy, and some limitations and/or problems to be solved are discussed.

Nomenclature

C = concentration of reactant [g-moles/l]
f = fraction of reactant converted [—]
k = reaction rate constant [l/g-moles·min]
N = impeller stirring rate [rev/min]
r = reaction rate [g-moles/l·min]
ϕ = volume fraction of dispersed phase in a stirred tank reactor [—]
τ = mean residence time of reactants in a stirred tank reactor [min]
ω_i = interaction rate of dispersed phase [l/min]

Literature cited

1) Madden, A. J. and G. L. Damerell: *A. I. Ch. E. Journal*, 8, 223 (1962)
2) Miller, R. S., J. H. Ralph, R. L. Curl and G. D. Towell: *A. I. Ch. E. Journal*, **9**, 196 (1963)
3) Rietema, K.: *Advances in Chem. Eng.*, **5**, 278 (1964)
4) Spielman, A. and O. Levenspiel: *Chem. Eng. Sci.*, **20**, 247 (1965)

PNEUMATIC CONVEYING OF SOLIDS THROUGH STRAIGHT PIPES*

HIROTAKA KONNO AND SHOZABURO SAITO
Dept. of Chem. Eng., Tōhoku Univ., Sendai

The pneumatic transport of solid particles in both horizontal and vertical pipes was studied using glass beads, copper spheres, millet and grass seeds, having diameters ranging from 0.1 to 1.0 mm. It was shown that the additional pressure drop and the particle velocity could be expressed by $\Delta P_s/L = 0.057\,(u_a/\sqrt{gD})\,m\rho_a$, and $u_s = u_a - u_t$, respectively, in the case of vertical transport.

In vertical transport, the copper spheres and glass beads were found to be densely distributed toward the wall of the pipe whereas higher concentration near the axis was observed for polystyrene particles.

The velocity profile of the air in the vertical pipe was symmetrical and was not appreciably affected by the addition of the particles. However, in the horizontal pipe, the velocity profile was asymmetric with respect to the pipe axis, and was found to be affected by the particle diameter, density, and the mass flow ratio of the air and the particles.

A simple impulsive model was used to explain the additional pressure drop in horizontal conduits, which was thought to be caused mainly by the collision between the particles and the surface of the pipe wall.

In a discussion of dispersed-phase flow, it is necessary to consider vertical and horizontal systems separately. In the previous paper[9], the pressure drop, the particle velocity and the particle distribution were measured in a horizontal pipe. In the present study, two vertical pipes were used to measure those quantities, and the air velocity profile was measured in both horizontal and vertical pipes.

Correlations for pressure drop in gas-solids transport lines have been presented in various papers[1,4~7,14,15] with widely differing results. From the experiment in the previous paper, it was found that the characteristics of dispersed solid flow were very sensitive to the experimental conditions, especially to the roughness of the surface of the pipe wall. To avoid uncertainty in defining the roughness of the pipe, a glass conduit having a smooth surface and spherical particles, such as glass beads, were used.

In the transport of solid particles in a horizontal conduit, for a fully developed flow, the additional pressure drop was considered to be brought about mainly by the collision between particles and the surface of the pipe wall. Therefore, a simple model was

* Received on June, 1, 1968
This article was presented at the 33rd annual meeting of Soc. Chem. Engrs. Japan. (1968)

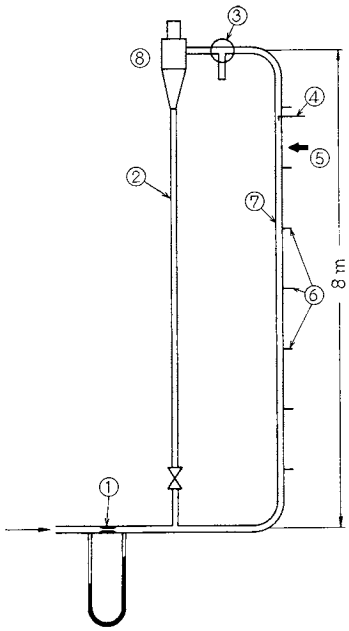

Fig. 1 Schematic diagram of experimental apparatus for vertical transport

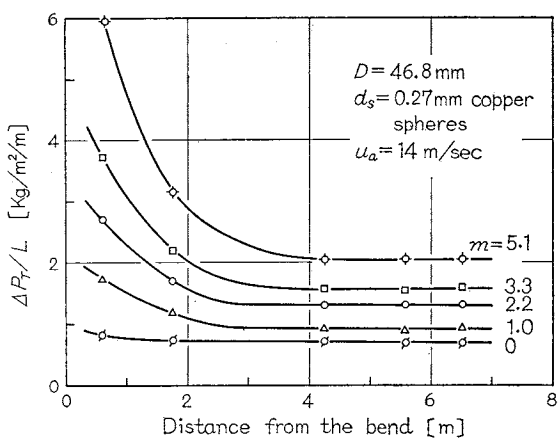

Fig. 2 Effect of particle acceleration on pressure drop in vertical transport

proposed based on the equations of impulsive motion. Experimental results were then compared with the theoretical calculations.

1 Experimental Procedure

The apparatus for vertical transport is shown schematically in **Fig. 1** and that for horizontal is the same as used in the previous investigation. The techniques to measure pressure drops and particle velocities were also described in detail in the previous paper.

Two glass pipes 8 m in length were used, one of 26.5 mm inside diameter and the other, 46.8 mm.

Air velocity profiles in both vertical and horizontal pipes with 46.8 mm inside diameter were measured by inserting a Pitot tube of 0.5 mm outside diameter into the stream of the dispersed solid flow. The pitot tube was placed at about 7 m from the bottom of the vertical section.

Table 1 Properties of the solid materials

Material	Density [kg/m³]	Geometric mean dia. [mm]	Geometric standard deviation	Free falling velocity in air [m/s]
Glass	2,500	0.12	1.25	0.95
		0.32	1.07	2.53
		0.52	1.10	4.10
		1.05	1.06	8.00
Copper	8,900	0.12	1.08	2.20
		0.27	1.11	5.00
		0.53	1.12	9.80
Hairy vetch	1,350	3.25	1.08	10.00
Millet	1,440	1.44	1.09	7.13

The solid particles used in this experiment were glass beads, copper spheres, millet and grass seeds (hairy vetch). The glass beads were graded by making use of the difference in their free-falling velocity in water, and the other materials were sieved with Tyler standard screens. Each sample of solid particles thus had a relatively uniform particle size. The physical properties of the materials are given in **Table 1.** The size was determined under microscope. The air velocities and the mass flow ratios of the solids to gas were varied from 8 to 20 m/sec and from 0 to 6, respectively.

The extent to which the flow is "developed" was measured by reading the pressure drops at several locations along the vertical section of the apparatus as shown in **Fig. 2.** The actual experimental runs were made in the region where the fully developed flow was maintained, as it was in the case of the previous investigation with the horizontal pipe.

For the materials and the air velocity studied, a length of about 4 m of the conduit was required to achieve the complete particle acceleration in the vertical transport experiment. About 9 m was required for horizontal transport, as shown in the previous paper.

2 Experimental Results

2-1 Flow Pattern of Particles

Two types of particle flow were observed in vertical transport, as also in the previous investigation in the horizontal pipes. One type was a flow comparatively parallel to the pipe axis, and the other was a random flow in which solid particles were violently colliding with the pipe wall. The correlations between pressure drop and mass flow ratio were not linear when particles were conveyed in random motion. The random flow was not always observed, even when the same particles and conduit were used. The causes of random flow are not at all clear at present.

These two types of flow showed large differences in pressure drop. In this paper, the investigation was made for parallel flow type alone, since it was difficult to reproduce the experimental conditions for random

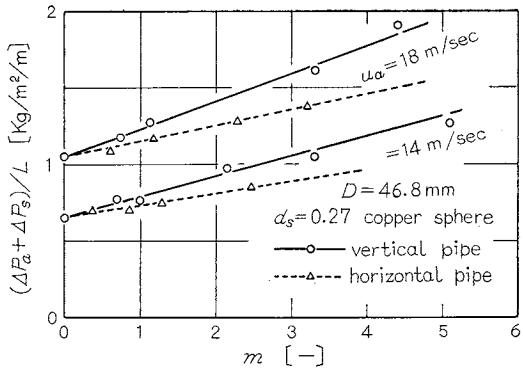

Fig. 3 Comparison of pressure drop for horizontal and vertical transport of copper spheres

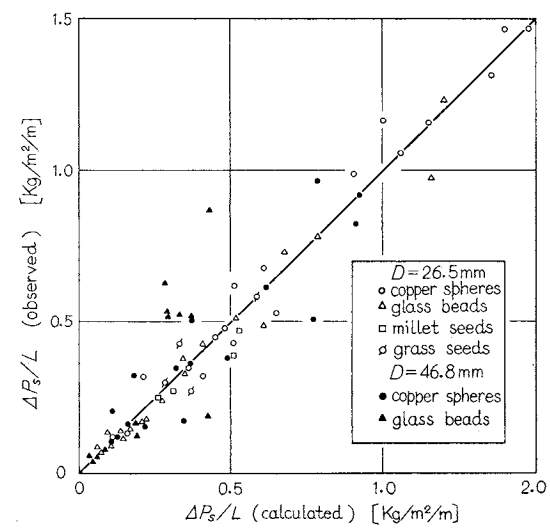

Fig. 4 Comparison of calculated and observed pressure drops in vertical transport

flow.

2-2 Pressure Drop

In the regions where the acceleration of the gas and solids is completed, the total pressure drop in the vertical pipe may be composed of the pressure drop due to the fluid friction ΔP_a, the solids static head ΔP_h, and the friction loss of solids ΔP_s. This can be expressed as follows;

$$\Delta P_T = \Delta P_a + \Delta P_s + \Delta P_h \quad \text{(for vertical pipe)} \qquad (1)$$

where ΔP_a was calculated by the Fanning equation, and ΔP_h can be estimated by the following equation;

$$\Delta P_h = L\rho_{ds} = L\frac{G_s}{Au_s}$$

Examples of pressure drops $(\Delta P_a+\Delta P_s)$ for the vertical pipe are given in **Fig. 3** and are compared with those for the horizontal pipe. The friction loss of solids ΔP_s in vertical flow always tended to be larger than that in horizontal flow.

Applying the Fanning equation to the flow of solids in the pipe, the pressure drop due to solid friction may be given as

$$\frac{\Delta P_s}{L} = \frac{2f_s u_s^2}{gD}\rho_{as} = \frac{2f_s u_s u_a}{gD}m\rho_a \qquad (2)$$

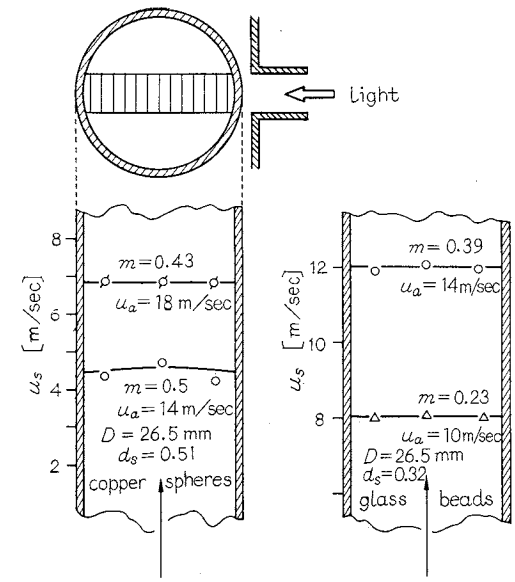

Fig. 5 Particle velocity profiles in vertical transport

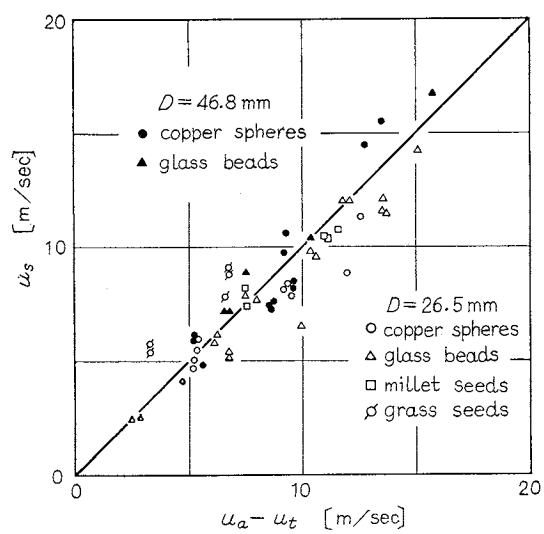

Fig. 6 u_s vs. (u_a-u_t) in vertical transport

From the experimental data, $2f_s u_s$ was found to be expressed as $5.7\times10^{-2}\sqrt{gD}$. Hence f_s becomes;

$$f_s = \frac{0.0285}{u_s/\sqrt{gD}} \qquad (3)$$

Combining this with the above Eq.(2), the following equation was obtained.

$$\frac{\Delta P_s}{L} = 5.7\times10^{-2}\frac{u_a}{\sqrt{gD}}m\rho_a \qquad (4)$$

A comparison of observed and calculated pressure drop from Eq.(4) is shown in **Fig. 4.**

2-3 Particle Velocities

Examples of particle velocities are shown in **Fig. 5.** According to this figure it is considered that the local axial particle velocities are comparatively uniform over the pipe cross section.

The mean value of the axial particle velocities is expressed approximately by the difference between the mean air velocity and free falling velocity of the par-

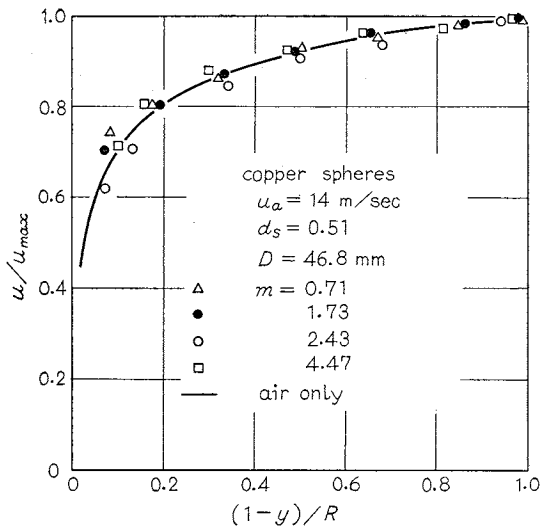

Fig. 7 Air velocity profiles in vertical transport

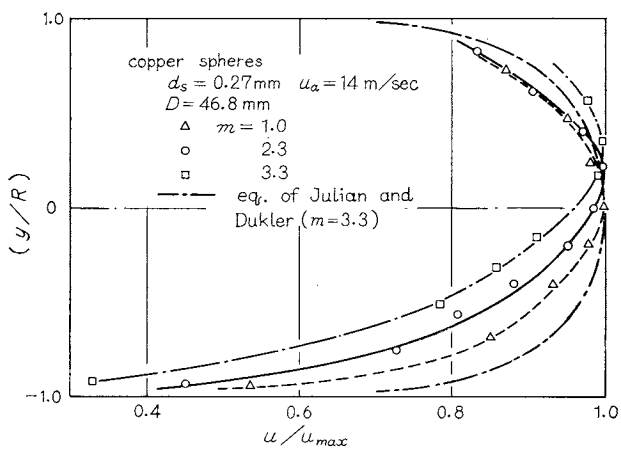

Fig. 8 Air velocity profiles in horizontal transport

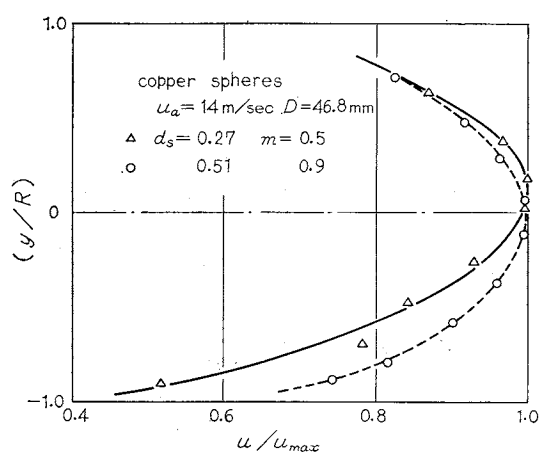

Fig. 9 Air velocity profiles in horizontal transport

ticles.

$$u_s = u_a - u_t \qquad (5)$$

Fig. 6 shows a plot of this relation.

2-4 Air Velocity Profiles in Pipes

In **Fig. 7** are shown the plots of air velocity profiles

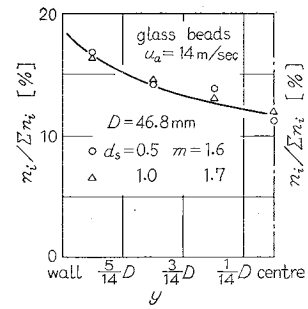

Fig. 10-a Particle distribution in vertical pipe (effect of particle diameter)

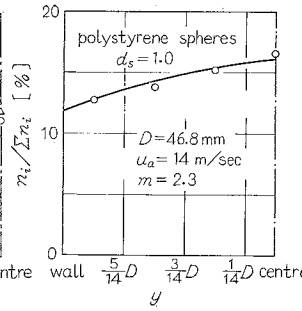

Fig. 10-b Particle distribution in vertical pipe

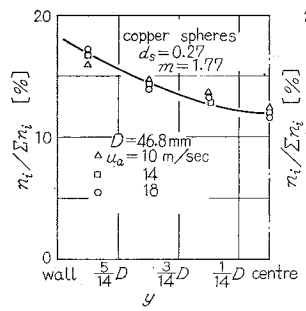

Fig. 10-c Particle distribution in vertical pipe (effect of air velocity)

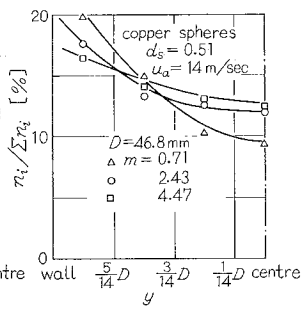

Fig. 10-d Particle distribution in vertical pipe (effect of mass flow ratio)

of dispersed solid flow in the vertical pipe. Air velocity profile was not affected by adding solid particles and satisfied the 1/7-th-power law. That is, the same results were obtained for the different experimental conditions of particle diameters, mean velocities and densities of particles.

In the horizontal conduit, air velocity profiles differ from those in the vertical conduit. Examples of the experimental data are presented in **Figs. 8** and **9.** The air velocity profile is not symmetrical with respect to the pipe axis. The location of maximum velocity in the pipe moved gradually upwards from the center of the pipe with increasing mass flow ratio. In the same mass flow ratio, a more asymmetrical velocity profile was obtained when smaller particles were used as shown in Fig. 9. But on both sides of the line of maximum velocity, air velocity profiles satisfied the 1/n-th-power law.

Recently, Julian and Dukler[8] proposed a new model for gas-solids flow systems. Their model was shown to fit the experimental data fairly well for pressure drop in horizontal transport in the previous paper. But asymmetrical profiles in the horizontal pipe as seen in Fig. 8 could not be explained by their eddy viscosity model.

2-5 Particle Distribution in Pipes

In the previous experiment, the distribution of particles in the direction of gravity in the horizontal pipe was observed to be expressed by an exponential function.

In the vertical pipe with 46.8mm inside diameter, measurements of the distribution of particles across the pipe cross-section were carried out, using a photographic technique.

The slit of light across the pipe as shown in Fig. 5 was divided into 7 sections by six vertical parallel planes set at equal distances. **Fig. 10** shows the ratio of the number of particles in each section to the total number of particles vs. the distance from the wall.

The distribution showed the particle concentration to be higher near the wall when copper and glass particles were conveyed, as seen in Fig. 10. However, for polystyrene particles (diameter=1.0mm), higher concentration near the axis was observed as shown in Fig. 10-b. This phenomenon has also been reported by Doig et al.[3] for glass particles having the diameter of 304 and 756 microns.

The cause of such a particle distribution cannot be explained, since the force on the particle is unknown at present. Figs. 10-a and 10-c show the effects of particle size and air velocity, respectively, to particle distribution.

Particle distribution in the pipe is more affected by mass flow ratio than by the particle size and air velocity. Mass flow ratio affects them as shown in Fig. 10-d. The higher the particle concentration becomes, the more uniform becomes the observed particle distribution.

3 Analytical Study of Additional Pressure Drop in Horizontal Pipe

At the present, the transverse force on the particle in vertical transport is not known. In horizontal transport, however, it is considered that this force on the particle is largely caused by gravitational force. Therefore in this section only the additional pressure drop in the horizontal pipe is considered.

When moving particles collide with the pipe wall, some of their kinetic energy will be lost[10,11,12]. The lost energy would have to be given back by the fluid in order to maintain steady state flow. That is, the additional pressure drop ΔP_s will balance the kinetic energy of the particles consumed by collision with the pipe wall.

The loss of energy may be expressed by the following equation ;

$$E = \frac{1}{2}M_s\{(v_{z0}^2 + v_{y0}^2) - (v_{z1}^2 + v_{y1}^2)\} + \frac{1}{2}I(\omega_0^2 - \omega_1^2) \quad (6)$$

Collision of particles to the pipe wall is discussed under the following assumptions.

i) Velocity component v_z is actually somewhat changed at collision, but v_z is assumed to be given back the velocity it had before the collision as soon as the particle collides with the wall.

Similarly, the velocity component in the cross section ($\sqrt{v_x^2+v_y^2}$), and the angular velocity (ω) are also given back their former states as soon as they change at collision.

These are based on the fact that most particles are observed to keep almost uniform velocity component v_z at any point and to be carried through the pipe without settling on the bottom surface of the pipe wall.

ii) The chance of the collision between the particles themselves is negligibly small. This was experimentally observed by high-speed cinephotographic pictures.

iii) The axis of rotation of the particle is at right angles to the trace of the particle motion and parallel to the tangential plane at the point of collision.

iv) The reflected particle moves in a gravitational field after the velocity of the particle is recovered according to assumption (i). Then the particle collides with the pipe wall again. The drag force on the moving particle is always neglected.

v) Initially, the particles are located at the height of the top of the horizontal pipe. The particles begin to fall in the gravitational direction with constant velocity v_z in the Z direction, constant angular velocity ω and zero initial velocity v_x and v_y.

As the reflection point of collision in the pipe can be considered to be on the tangential plane, the collision in the three dimensional field was treated in the same way as in the two dimensional field which is discussed in Appendix.

By experiments the coefficients of restitution e and kinetic friction μ were estimated at about 0.9 and 0.4, respectively. The coefficient of static friction μ_s is estimated at 0.8 from literature[13].

The particle velocity component in the Z direction, v_z, was determined from the empirical equation in the previous paper.

The loss of energy of the particles was calculated by using a digital computer HITAC-5020 using the following conditions for the 80 particles which were located at the same intervals in X direction ; air velocities, 8 to 20m/sec ; the diameter of the glass beads, 0.5mm ; mass flow ratio, 0.6 ; and the inside diameter of glass pipe, 46.8mm.

In **Fig. 11**, the calculated pressure drop is plotted against the angular velocity. In **Fig. 12** is shown the pressure drop vs. air velocity.

The calculated pressure drop agrees comparatively well with the measured value at the angular velocity of about 2000r.p.s..

Смолцвіров[2] expressed that a moving particle in the pipe was rotating at 1000~3000r.p.s.. This observation could be taken to suggest that our simple impulsive model is approximately appropriate in explaining one of the main causes of the additional pressure drop in the horizontal transport of a gas-solid dispersion in smooth pipe.

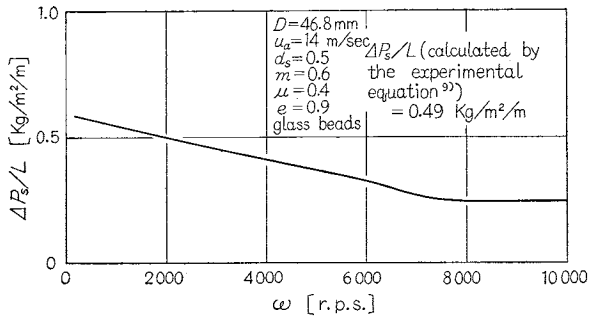

Fig. 11 Calculated pressure drop (effect of angular velocity)

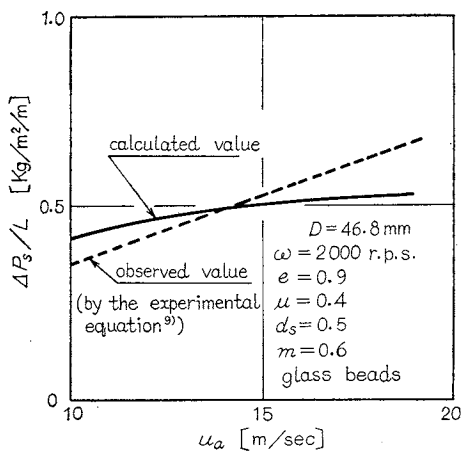

Fig. 12 Calculated pressure drop (effect of air velocity)

Conclusion

A study was made of the transport of solid particles through horizontal and vertical pipes by an air stream. Air velocity and mass flow ratio were varied from 8 to 20 m/sec and from 0 to 6, respectively.

In vertical flow, the additional pressure drop could be expressed by Eq. (4) and the particle velocity by $u_s = u_a - u_t$. In vertical transport of copper and glass particles, the particles were observed to be distributed in decreasing density from the wall towards the center, but polystyrene particles showed the inverse distribution. The air velocity profiles in the presence of dispersed solids were measured both in horizontal and vertical conduits. For the vertical conduits, they were the same as that in the absence of solid particles and were well represented by the 1/7-th-power law. For the horizontal conduit, they showed an asymmetrical profile with respect to the pipe axis.

Finally it was explained by the simple impulsive model that the additional pressure drop in the horizontal pipe might be caused mainly by the collision between the particle and the surface of the pipe wall.

Appendix

Impulsive Motion in Two-Dimensional Field

Equations of impulsive motion are given as follows,

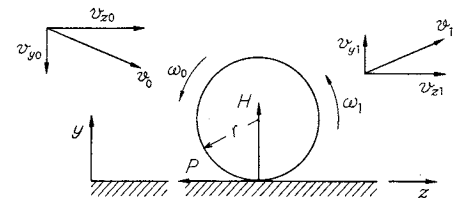

Fig. 13 Two-dimensional coordinate system of a single spherical solid particle colliding with the wall

$$M_s(v_{z1} - v_{z0}) = -P \quad \text{for } Z \text{ direction} \qquad \text{(i)}$$
$$M_s(v_{y1} - v_{y0}) = H \quad \text{for } Y \text{ direction} \qquad \text{(ii)}$$
$$I(\omega_1 - \omega_0) = -P \cdot r \qquad \text{(iii)}$$
$$v_{y1} = -e v_{y0} \qquad \text{(iv)}$$

Depending upon the condition of the colliding, either Eq. (v) or (v') has to be used.

For the particle slipping on the wall;

$$P = \mu H \qquad \text{(v)}$$

For the particle not slipping on the wall;

$$v_{z1} + r\omega_1 = 0 \qquad \text{(v')}$$

where as illustrated in **Fig. 13**, H and P are the impulsive force, I is the moment of inertia of the particle, and ω is the angular velocity of the particle.

If it is assumed that the particle does not slip during contact with the wall, the impulsive force H is calculated by using Eqs. (i) to (iv) and (v').

The no-slip assumption will be satisfied if $P \leqq \mu_s H$ where μ_s is the coefficient of static friction, and the condition (v') has to be used to follow the motion of the particle. The condition (v) where there is a slip on the wall will have to be used if $P > \mu_s H$.

The solution for the case of no-slip is given by the following equations;

$$\left.\begin{aligned} v_{z1} &= \frac{5v_{z0} - 2\omega_0 r}{7}, \quad v_{y1} = -e v_{y0}, \\ \omega_1 &= \frac{2\omega_0 r - 5v_{z0}}{7r}, \quad H = M_s(1+e)(-v_{y0}), \\ P &= \frac{2}{7} M_s(v_{z0} + r\omega_0) \end{aligned}\right\} \qquad \text{(vi)}$$

For the spherical particle, I is given by $2/5 M_s r^2$. In the case of slipping condition,

$$\left.\begin{aligned} v_{z1} &= v_{z0} + (1+e)v_{y0}, \quad v_{y1} = -e v_{y0} \\ \text{and} \\ \omega_1 &= \omega_0 + \frac{5\mu(1+e)v_{y0}}{2r} \end{aligned}\right\} \qquad \text{(vii)}$$

If the velocity and the angular velocity of the particle before collision are given, the velocities of the particle after the collision can be calculated from Eq. (vi) or Eq. (vii).

Acknowledgment

The authors extend their sincere thanks to Professor Siro Maeda for valuable suggestions and criticisms, and express their appreciation to Mr. Hiroyuki Kondō and Mr. Saburō Takahashi for their assistance in the experimental investigation. They are grateful to the Science Research Foundation of the Ministry of Education in Japan for its support of this study.

Nomenclature

A	= cross sectional area of pipe	[m²]
D	= pipe diameter	[m]
d_s	= particle diameter	[m]

e	= coefficient of restitution	[—]
f_s	= Fanning friction factor for the solid particle	[—]
G_s	= solid mass velocity	[kg/sec]
G_a	= air mass velocity	[kg/sec]
H	= impulsive force for Y direction	[Kg·sec]
I	= moment of inertia of particle	[kg·m]
L	= pipe length	[m]
M_s	= particle mass	[kg]
m	= mass flow ratio $=G_s/G_a$	[—]
n_i	= local number of particles in unit volume	[1/cc]
P	= impulsive force for Z direction	[Kg·sec]
ΔP_a	= pressure drop due to fluid friction	[Kg/m^2]
ΔP_h	= solid static head	[Kg/m^2]
ΔP_s	= additional friction loss	[Kg/m^2]
ΔP_T	= total pressure drop	[Kg/m^2]
R	= pipe radius	[m]
r	= particle radius	[m]
u	= local air velocity	[m/sec]
u_a	= mean air velocity	[m/sec]
u_{max}	= maximum air velocity	[m/sec]
u_s	= solid velocity	[m/sec]
u_t	= free falling velocity of particle in air	[m/sec]
v_x	= velocity component of X direction	[m/sec]
v_y	= velocity component of Y direction	[m/sec]
v_z	= velocity component of Z direction	[m/sec]
y	= distance from pipe axis	[m]
X	= direction at right angles to Y and Z	
Y	= opposite gravitational direction	
Z	= longitudinal direction of the pipe	
μ	= coefficient of kinetic friction	[—]
μ_s	= coefficient of static friction	[—]
ρ_a	= air density	[kg/m^3]
ρ_{ds}	= dispersed density	[kg/m^3]
ρ_s	= solid density	[kg/m^3]
ω	= angular velocity of the particle	[rad/sec]

Subscript
0 = before collision
1 = after collision

Literature Cited

1) Belden, D. H. & L. S. Kassel: *Ind. Eng. Chem.*, **41**, 1174 (1949)
2) Смолцвірев, A. E.: Paipu Yusō (translated in Japanese by Z. Sotoo & M. Nagai) Gijutsu Shoin (1963)
3) Doig, I. D. & G. H. Roper: *Ind. Eng. Chem., Fundamentals*, **6**, 247 (1967)
4) Hariu, O. H. & M. C. Molstad: *Ind. Eng. Chem.*, **41**, 1150 (1949)
5) Hinkle, B. L.: Ph. D. thesis. Georgia Inst. of Tech. (1953)
6) Iinoya, K. & K. Gotō: *Kagaku Kōgaku (Chem. Eng., Japan)*, **27**, 12 (1963)
7) Jōtaki, T. & H. Mori: *Trans. J. S. M. E.*, **33**, 1617 (1967)
8) Julian, F. M. & A. E. Dukler: *A. I. Ch. E. Journal*, **11**, 853 (1965)
9) Konno, H. S. Saitō & S. Maeda: *Kagaku Kōgaku (Chem. Eng., Japan)*, **31**, 243 (1967)
10) Mori, Y., A. Suganuma & H. Sadotomo: Preprint of 31 st annual meeting of Soc. Chem. Engrs. Japan
11) Muschelknautz, E.: *V. D. I. Forschungsheft*, 476 (1959)
12) Ranz, W. E., G. R. Talandis & B. Gutterman: *A. I. Ch. E. Journal*, **6**, 124 (1960)
13) Tabor, D. & F. P. Bowden: *Kotai no Masatsu to Junkatsu* (translated in Japanese by M. Sōda) Maruzen (1964)
14) Uematsu, T. & T. Kanno: *Trans. J. S. M. E.*, **27**, 1748 (1961)
15) Vogt, E. G. & R. R. White: *Ind. Eng. Chem.*, **40**, 1731 (1948)

POWER REQUIREMENTS IN THE AGITATION OF NON-NEWTONIAN FLUIDS*

NOBUO MITSUISHI AND NOBUYUKI HIRAI

Department of Chemical Engineering, Kyushu University, Fukuoka, Japan

A modified Reynolds number in the agitation, based on the Ellis and Sutterby models of three rheological constants for non-Newtonian fluids, is defined in the way that the relation between friction factor and Reynolds number in the case of non-Newtonian pipe flow may be the same as that in the case of Newtonian pipe flow.

Introducing this modified Reynolds number, the same correlation of the power requirements can be applied to both experimental results of Newtonian and non-Newtonian fluids with various types of impellers.

1. Introduction

Agitation, which is one of the most important unit operations, is not easy to approach theoretically and quantitatively. The measurement of power requirements in the agitation is, however, comparatively easy, and the estimation of power consumption for Newtonian fluids is now possible except for some special cases. On the contrary, studies of power requirements in the agitation of non-Newtonian fluids are making slow progress. Such works have been carried out, by Metzner et al.[8,9], Calderbank and Moo-Young[1,2], and others[3,4,6,12]. In many of these studies, a power-law model with two constants has been used to describe the rheological properties of non-Newtonian fluids. However, the power-law model cannot express the properties of non-Newtonian fluids in a wide range

* Received on May 29, 1968
The first annual meeting in autumn, Soc. Chem. Eng. Japan, Octorber 14, 1967